WILEY AJH

RESEARCH ARTICLE

Plasma proteomics identifies a 'chemokine storm' in idiopathic multicentric Castleman disease

Sheila K. Pierson[1] | **Aaron J. Stonestrom[2]** | **Dustin Shilling[1]** | **Jason Ruth[3]** | **Christopher S. Nabel[3]** | **Amrit Singh[4]** | **Yue Ren[1]** | **Katie Stone[5]** | **Hongzhe Li[1]** | **Frits van Rhee[5]** | **David C. Fajgenbaum[1]** (iD)

[1]University of Pennsylvania, Philadelphia, Pennsylvania; [2]Hospital of the University of Pennsylvania, Philadelphia, Pennsylvania; [3]Castleman Disease Collaborative Network, Boston, Massachusetts; [4]University of British Columbia, Vancouver, Canada; [5]University of Arkansas for Medical Sciences, Little Rock, Arkansas

Correspondence
David C. Fajgenbaum, Hospital of the University of Pennsylvania, 3400 Spruce St, S05094 Silverstein, Division of Translational Medicine and Human Genetics, Philadelphia, PA, 19104.
Email: davidfa@pennmedicine.upenn.edu

Human Herpesvirus-8 (HHV-8)-negative/idiopathic multicentric Castleman disease (iMCD) is a poorly understood disease involving polyclonal lymphoproliferation with dysmorphic germinal centers, constitutional symptoms, and multi-organ failure. Patients can experience thrombocytopenia, anasarca, reticulin fibrosis, renal dysfunction, organomegaly, and normal immunoglobulin levels, –iMCD-TAFRO. Others experience thrombocytosis, milder effusions, and hypergammaglobulinemia, –iMCD-Not Otherwise Specified (iMCD-NOS). Though the etiology is unknown in both subtypes, iMCD symptoms and disease progression are believed to be driven by a cytokine storm, often including interleukin-6 (IL-6). However, approximately two-thirds of patients do not respond to anti-IL-6 therapy; alternative drivers and signaling pathways are not known for anti-IL-6 nonresponders. To identify potential mediators of iMCD pathogenesis, we quantified 1129 proteins in 13 plasma samples from six iMCD patients during flare and remission. The acute phase reactant NPS-PLA2 was the only significantly increased protein ($P = .017$); chemokines and complement were significantly enriched pathways. Chemokines represented the greatest proportion of upregulated cytokines, suggesting that iMCD involves a chemokine storm. The chemokine CXCL13, which is essential in homing B cells to germinal centers, was the most upregulated cytokine across all patients (log2 fold-change = 3.22). Expression of CXCL13 was also significantly increased in iMCD lymph node germinal centers compared to controls in a stromal meshwork pattern. We observed distinct proteomic profiles between the two iMCD-TAFRO patients, who both failed anti-IL-6-therapy, and the four iMCD-NOS patients, in whom all three treated with anti-IL-6-therapy responded, suggesting that differing mechanisms may exist. This study reveals proteomic differences between flare and remission and the potential to molecularly define iMCD subgroups.

1 | INTRODUCTION

Human Herpesvirus (HHV)-8-negative, idiopathic multicentric Castleman disease (iMCD) is a polyclonal lymphoproliferative disorder with an unknown etiology. Approximately 1000 individuals of all ages are diagnosed with iMCD each year in the USA,[1] and 35%-45% of patients die within 5 years of diagnosis.[2–4] Patients experience heterogeneous clinical and laboratory abnormalities including constitutional symptoms, anemia, anasarca, renal failure, hypoalbuminemia, thrombocytopenia or thrombocytosis, and multicentric lymphadenopathy. Characteristic histopathological features of the enlarged lymph nodes include dysmorphic (atrophic or hyperplastic) germinal centers, hypervascularization, polyclonal lymphoproliferation, and/or polytypic plasmacytosis.[5]

Recently, a new clinical subtype of iMCD has been described involving thrombocytopenia, anasarca, fibrosis of bone marrow, renal dysfunction, organomegaly (iMCD-TAFRO), and normal immunoglobulin levels.[6,7] Other iMCD patients, who do not have TAFRO features (herein referred to as iMCD-Not Otherwise Specified or iMCD-NOS), more often demonstrate thrombocytosis, hypergammaglobulinemia, and less severe fluid accumulation.[8]

Similar clinical and histopathological changes that occur in iMCD also occur in HHV-8-positive MCD in which the HHV-8 virus replicates in lymph node plasmablasts and initiates a cytokine storm driving polyclonal lymphoproliferation and systemic symptoms.[9] Likewise, a cytokine storm—the uncontrolled release of proinflammatory cytokines[10]—is presumed to drive iMCD pathogenesis. However, the etiology,

signaling pathways, dysregulated cell types, and composition of the cytokine storm, including the various families of cytokines, such as interleukins and chemokines, are not known in iMCD. Chemokines regulate leukocyte migration, lymphoid tissue organization, innate and adaptive immunity, angiogenesis, and immune system development, whereas interleukins are often involved in stimulating immune responses, such as inflammation.

Several lines of evidence suggest that excess interleukin-6 (IL-6), a cytokine that promotes B cell and plasma cell growth, plays an important role in symptoms and disease progression in many iMCD patients.[11,12] Anti-IL-6 monoclonal antibodies (mAb) tocilizumab (anti-IL-6 receptor) and siltuximab (anti-IL-6) have been approved for iMCD in various regions of the world.[5,13,14] However, approximately two-thirds of iMCD patients did not respond to IL-6 blockade with siltuximab in the registrational trial,[14] and, of the 35 siltuximab nonresponders in the study, more than one-half had normal IL-6 levels during active disease (<5 pg/mL).[12] In agreement, a recent study of serum cytokines found that more than one-half of the 17 iMCD patients examined had undetectable IL-6 levels during flare.[15] These results suggest that IL-6 independent pathways may be driving disease pathogenesis in a portion of iMCD patients. Current treatment options for these patients include corticosteroids, rituximab, and cytotoxic chemotherapies, which have limited efficacy and significant toxicity in iMCD.[16] Efforts to identify new treatment strategies for patients who do not respond to anti-IL-6 therapy are limited by a poor understanding of iMCD pathogenesis.

Here, we performed for the first time unbiased, systematic quantification of plasma proteins in six iMCD patients' matched flare and remission samples using SomaLogic SOMAscan® to generate insights into iMCD pathogenesis.

2 | METHODS

2.1 | Patients and sample collection

All patients consented to the research, which was approved by the University of Arkansas for Medical Sciences Institutional Review Board. Clinical data were collected as part of routine care. Between 2007 and 2016, peripheral blood samples were collected from six patients whose diagnoses are consistent with the iMCD diagnostic criteria.[5] One sample during flare (defined as C-Reactive Protein (CRP) > 10 mg/L and the presence of at least two iMCD-related minor diagnostic criteria[5]) and one sample during remission (defined as CRP < 10 mg/L and less than two minor diagnostic criteria[5]) were collected from each patient. An additional sample was collected for patient 6 during a subsequent flare, which occurred three years after the first flare. In total, 13 samples collected from six iMCD patients were analyzed.

The demographic and disease characteristics of the six iMCD patients are presented in Supporting Information Table S1. Median age at diagnosis was 44.5 years, similar to previous reports.[16] One patient is female (16.7%). Five of six patients are white (83.3%), and one patient is black (16.7%). Patients 1–4 are iMCD-NOS, whereas patients 5–6 are iMCD-TAFRO. Five of the six patients were treated with anti-

IL-6-therapy (siltuximab or tocilizumab) during their disease course (Supporting Information Table S2). Of those treated, patients 1–3 responded to treatment and patients 5–6 did not respond. At the time of flare sample collection, patients 5 and 6 (flare 1) were on anti-IL-6 therapy, and at the time of remission sample collection, patients 1, 2, 3, and 5 were on anti-IL-6 therapy. Complete treatment information is listed in Supporting Information Table S2. Plasma was isolated following standard protocols, stored at −80°C, and shipped in 150 mL aliquots overnight on dry-ice to SomaLogic, Inc (Boulder, Colorado) for analysis.

2.2 | High-throughput protein quantification and analysis

SomaLogic's SOMAscan®, a multiplexed, aptamer-based binding-assay, which has been described in depth previously,[17] was used to quantify the relative levels of 1129 proteins. Briefly, the SOMAscan assay uses Slow-Off-rate Modified Aptamer (SOMAmer) reagents, which are chemically modified nucleotides, to bind and quantify target proteins in relative fluorescent units directly proportional to the amount of target protein in the sample.

Data analyses were performed using R version 3.4.2.[18] Data were normalized by log2 transformation. Fold-change was calculated as the log2 (flare/remission) for each patient. Both of the patient 6 flare samples, labeled as 6.1 and 6.2, were compared to the remission sample. Protein function was assigned according to the UniProt molecular function annotation. For comparison of flare and remission and of clinical subgroups, P values were calculated using Linear Models for Microarray and RNA-Seq data (LIMMA)[19] and adjustment for multiple-hypothesis testing was performed using the method of Benjamini and Hochberg (false discovery rate (FDR) < .05).[20]

Gene-set enrichment analyses based on the Reactome Pathway Database and Kyoto Encyclopedia of Genes and Genomes (KEGG) database and drug enrichment analysis based on the Library of Integrated Network-Based Cellular Signatures (LINCS) 1000 database were performed using Enrichr.[21,22] The LINCS 1000 database was used to identify compounds that decrease gene expression of upregulated proteins. Ingenuity® Pathway Analysis (IPA) software was used for gene-set enrichment and pathway analyses. Enriched gene-sets identified among upregulated and/or downregulated proteins were compared against enriched gene-sets identified among the background of 1129 quantified proteins for all gene-set enrichment analyses. When appropriate, fold-enrichment ratio and a one-sided Fisher's Exact P value were calculated for comparison. A P value < .05 was considered significant, unless otherwise noted. A combined score, calculated by the log (P value)*z-score was used to rank the most significant compounds. Data analysis was performed by SKP, AJS, DS, AS, YR, HL, and DCF, and all authors had access to the primary clinical data.

2.3 | Immunohistochemistry

Immunohistochemistry (IHC) staining of formalin fixed paraffin embedded lymph node tissue from each iMCD patient and five sentinel lymph

nodes from breast cancer patients with no evidence of metastasis was performed at the Pathology Core at the Children's Hospital of Philadelphia. Slides were generated at 5μm thickness. Epitope retrieval was done for 20 minutes with E2 retrieval solution (Leica Biosystems). IHC was performed on a Leica Bond Max automated staining system (Leica Biosystems) using the Bond Intense R staining kit (Leica Biosystems DS9263). Polyclonal rabbit anti-CXCL13 (AF801, R&D Systems) was used at a 1:500 dilution and an extended incubation time of 1 hour at room temperature. Avidin Biotin Blocking was added (Vector Labs SP-2001) and a Peptide Blocking step was included (DAKO X0909). Slides were digitally scanned at 20× magnification on an Aperio ScanScope CS-O slide scanner (Leica Biosystems) and analyzed offline using Aperio ImageScope and Image Analysis Toolkit software (color deconvolution v9 algorithm).

3 | RESULTS

3.1 | iMCD flare and remission samples have distinct proteomic profiles

To visualize patterns in proteomic alterations that occur during iMCD flares, we performed principal component analysis (PCA) on all 13 samples (Figure 1A). The first principal component (PC1) did not clearly separate based on clinical subtype or disease state. The second principal component (PC2), which explained 13.9% of variance, separated flare and remission samples. Six of seven flare samples demonstrated a greater value on the PC2 component axis than all remission samples, and each flare sample demonstrated a greater PC2 value than its respective remission sample. To better understand the proteomic alterations that occur during flare, we plotted the 25 proteins contributing the most to PC2 based on absolute value of the features in the loading vector (Figure 1B). Hemoglobin and Serum Amyloid A (SAA) contributed the most to PC2. Hemoglobin was the most downregulated protein across all patients, which is consistent with anemia that occurs during flare. SAA, a cytokine-induced acute phase reactant produced by the liver, was the upregulated protein that contributed the most to differentiating flare from remission. Other acute phase reactants, such as Haptoglobin, CRP, Non-Pancreatic Secretory Phospholipase A2 (NPS-PLA2), and Complement 3b (C3b) were also among the top 10 strongest contributors to PC2. Five of the remaining top 25 contributing proteins demonstrate cytokine or chemokine activity, including Tissue Inhibitor of Metalloproteases-1 (TIMP-1), chemokine C-X-C motif chemokine ligand 13 (CXCL13), C-C motif ligand (CCL) 23 (CCL23), CCL21, and CCL14.

To visualize proteins significantly different in flare compared to remission across all iMCD patients, we performed a LIMMA modeling analysis of the log2 fold-change of all proteins and produced a volcano plot of the results (Figure 1C). However, only one protein, the acute phase reactant, NPS-PLA2, reached statistical significance after adjustment when compared across all iMCD patients ($P = .017$). In summary, iMCD flare and remission samples have distinct proteomic profiles involving consistent trends in acute phase reactants, cytokines, and chemokines between flare and remission.

3.2 | Pathways involving cytokines, chemokines, and complement are the most enriched during iMCD flare

As only one individual protein reached statistical significance across all iMCD patients when comparing flare to remission samples, we turned to gene-set enrichment analyses to identify gene-sets that are significantly altered during flare. Using KEGG gene-set database, we analyzed all proteins with at least a 2-fold mean increase across all patients during flare (list of >2-fold-change proteins available in Supporting Information Table S3). This analysis identified 14 significant KEGG gene-sets; cytokine-cytokine receptor interaction, chemokine signaling pathway, and complement and coagulation cascades were the top 3 gene-sets by combined score. To address the possibility that the set of 1129 proteins quantified through SOMAscan® was itself enriched for cytokine and chemokine pathways, we compared the results to the background set of all SOMAscan® proteins quantified. Chemokine signaling pathway and complement and coagulation cascades remained significantly enriched ($P = .03$ and $P = .04$, respectively), and the P value for cytokine-cytokine receptor interaction was .09 (Supporting Information Table S4), which confirmed enrichment of these pathways among the most upregulated proteins. We repeated gene-set analyses using the Reactome database. Gene-sets enriched at least 2-fold relative to the background set of all SOMAscan® proteins included cytokine signaling, such as G-protein coupled receptors and IL-1, −4, −10, and −13 signaling, chemokine signaling, and the complement cascade (Supporting Information Table S5). Results from both databases are consistent with involvement of cytokine and chemokine signaling and complement activation in iMCD flare.

3.3 | Chemokines are the most upregulated family of cytokines during iMCD flare

Given the enrichment of cytokine signaling and the generally accepted model of iMCD as a cytokine storm,[23] we performed additional analyses to investigate which cytokines were most elevated. Of the 120 cytokines measured by the SOMAscan® platform the average fold-change of chemokines was significantly higher than interleukins ($P = .048$) and other cytokines ($P = .025$) (Figure 2A, Supporting Information Table S6). Chemokines represented six of the eight cytokines that exceeded 2-fold upregulation. Further, nearly one-half of the quantified chemokines (43.6%) were represented among the top quartile, which was significantly greater than interleukins (11.1%, $P = .006$) or other cytokines (18.5%, $P = .008$). The three chemokines that were most upregulated during flare were CXCL13 (or B Lymphocyte Chemoattractant (BLC)), CCL23 (or Myeloid Progenitor Inhibitory Factor 1-1 (MPIF-1)), and CCL21 (or 6CKine). In contrast to the increased abundance of chemokines, relatively few interleukins were upregulated during iMCD flare. IL-6 was the most upregulated interleukin on average. However, this result is confounded by patients receiving anti-IL-6-therapy, which is known to increase circulating IL-6 levels.[24] The highest flare IL-6 level was found in the only patient (patient 5) who was receiving anti-IL-6-therapy during the flare draw, and the highest remission IL-6 levels were found in the patients on anti-IL-6-therapy. Given the potential bias of anti-IL-6 therapy, we removed samples obtained during anti-IL-6-
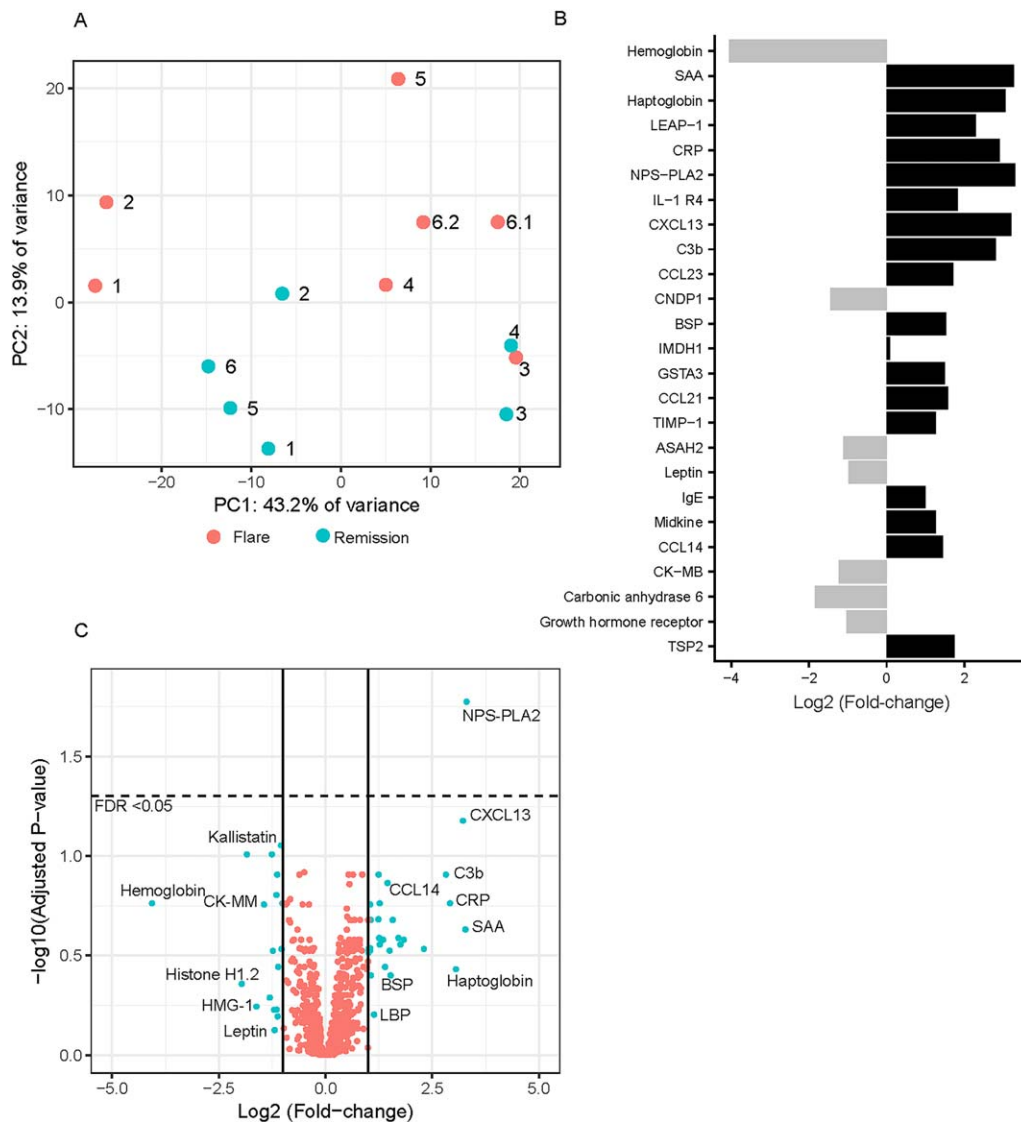
FIGURE 1 Proteomic alterations during iMCD flare. (A) Principal component analysis of all iMCD samples ($N = 13$). PC2, which accounted for 13.9% of variance, separated flare samples from remission. (B) Log2 fold-change of the top 25 proteins contributing to PC2; top contributory proteins consist of acute phase reactants, cytokines, and chemokines. (C) Volcano plot showing the log2 fold-change against the $-$log10 adjusted P value following LIMMA analysis. One protein (NPS-PLA2) reached statistical significance (horizontal line) following adjustment. Proteins in blue have >2-fold-change (log2 fold-change of -1.0 and 1.0, delineated by vertical lines) or are significantly elevated ($-$log10 (Adjusted P value) > 1.301, delineated by horizontal line) between flare and remission. Fifteen select proteins are identified by name. (Abbreviations: BSP: Bone sialoprotein 2; C3b: Complement C3b; CCL14: C-C motif chemokine 14; CK-MM: Creatine kinase M-type; CRP: C-reactive protein; HMG-1: High mobility group protein B1; LBP: Lipopolysaccharide-binding protein; NPS-PLA2: Phospholipase A2, membrane associated; SAA: Serum amyloid A-1 protein; FDR: False discovery rate) [Color figure can be viewed at wileyonlinelibrary.com]

therapy and calculated a log2-fold-change for each of the remaining flare samples (patients 1, 2, 3, 4, 6 (flare 2)) relative to the average of the remaining remission samples (patients 4, 6). Patients 1 and 2 had greater than 3-fold increased IL-6, while patients 3, 4, and 6 had less than 50% change. These results suggest that the cytokine storm observed in iMCD includes significant upregulation of chemokines.

3.4 | CXCL13 expression is elevated in iMCD lymph node tissue

To identify a potential cellular source of the elevated circulating CXCL13, we performed immunohistochemistry on iMCD lymph node tissue from each patient prior to iMCD treatment. Compared to sentinel lymph node tissue from breast cancer patients without evidence of metastasis (control), germinal centers in iMCD tissue demonstrated significantly increased medium ($P = .047$) and strong ($P = .022$) staining and significantly decreased weak staining ($P = .047$) (Figure 2B-D). CXCL13 reactivity appears in both a diffuse, meshwork pattern and a punctate pattern in the germinal center region, likely representing follicular dendritic cells (FDCs) and T follicular helper (TFh) cells, respectively. These findings suggest that lymph node tissue may be the source of elevated levels of circulating CXCL13 during iMCD flare.
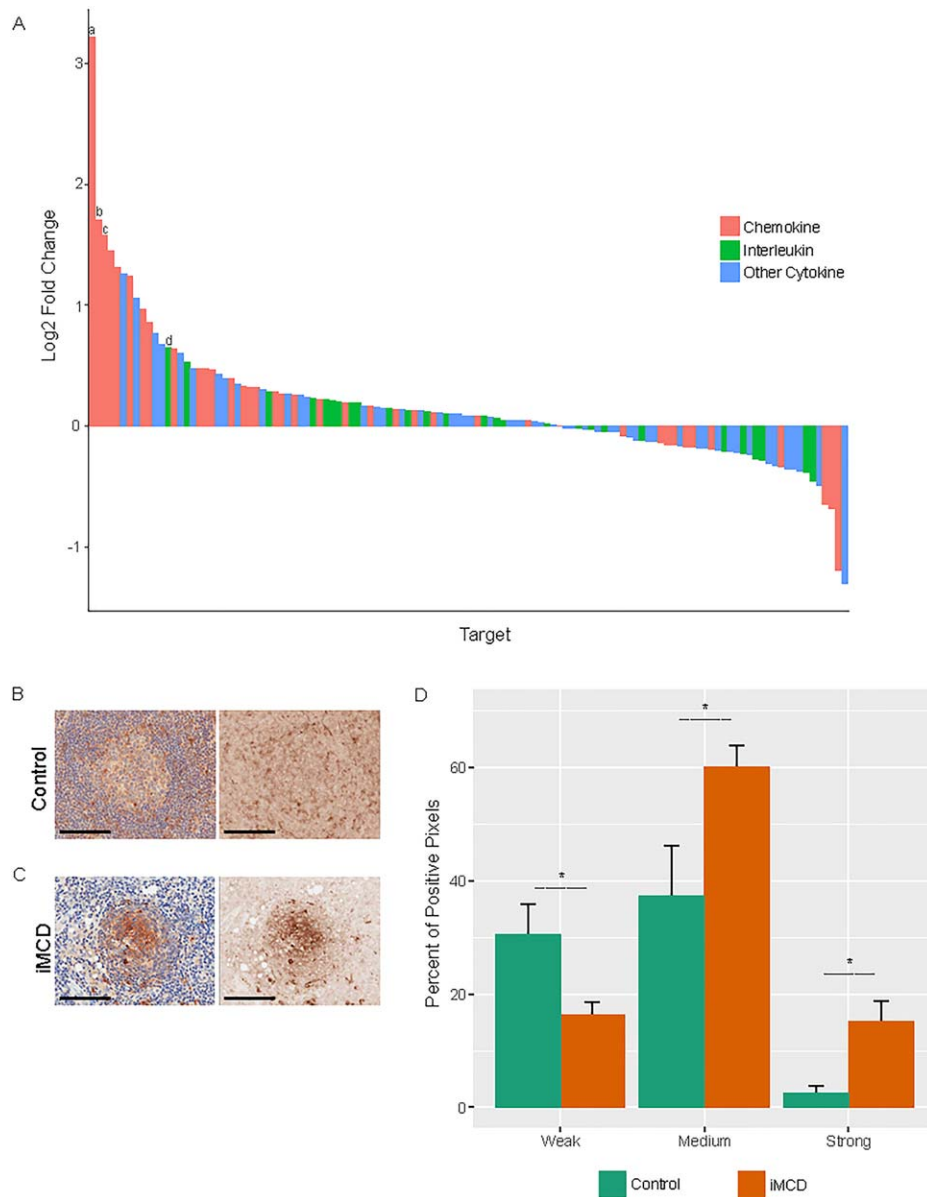
FIGURE 2 Chemokines are the most upregulated type of cytokine, and the most upregulated plasma chemokine, CXCL13, demonstrates elevated expression in iMCD lymph node tissue. (A) Bar plot showing mean log2 fold-change of all chemokines ($N = 39$), interleukins ($N = 27$), and other cytokines ($N = 54$) quantified by SOMAscan®. Mean fold-change among chemokines was significantly greater than that of interleukins or other cytokines ($P = .048$ and $P = .025$, respectively). CXCL13 was the most upregulated cytokine (log2 fold-change 3.22), followed by CCL23 (log2 fold-change 1.71) and CCL21 (log2 fold-change 1.57). IL-6 was the top upregulated interleukin (log2 fold-change 0.65). (B) High power image of a representative germinal center from a sentinel lymph node from a breast cancer patient with no evidence of metastasis (Control); (C) high power image of a representative germinal center from an iMCD lymph node, which was resected prior to receiving any iMCD therapy (iMCD) (bar = 100 μm). Tissue was immunostained with an antibody against CXCL13. (D) Quantification of germinal center CXCL13 staining intensity, as the percentage of pixels, for six iMCD (orange) and five control (green) lymph nodes. Aperio ImageScope was used for all analyses. ([a]CXCL13; [b]CCL23; [c]CCL21; [d]IL-6; *$P < .05$) [Color figure can be viewed at wileyonlinelibrary.com]

3.5 | Bioinformatic analyses reveal distinct proteomic profiles between groups associated with clinical subtype and anti-IL-6 response

To investigate whether patterns of proteomic alteration differ across patients, we performed a PCA of the log2 fold-change values for all proteins for each flare-remission pair (Figure 3A). Strikingly, PC1 (accounting for 62.7% of the variance) separated patients by clinical

subtype (iMCD-TAFRO vs iMCD-NOS) and response to anti-IL-6-therapy. Both iMCD-TAFRO cases did not respond to anti-IL-6-therapy whereas the three iMCD-NOS patients treated with anti-IL-6-therapy responded (one iMCD-NOS patient never received anti-IL-6-therapy). We next analyzed correlations between samples by comparing all 1129 proteins (Figure 3B). While there was positive correlation across the proteomes within the iMCD-TAFRO and iMCD-NOS groups, the proteomes of iMCD-TAFRO patients were negatively
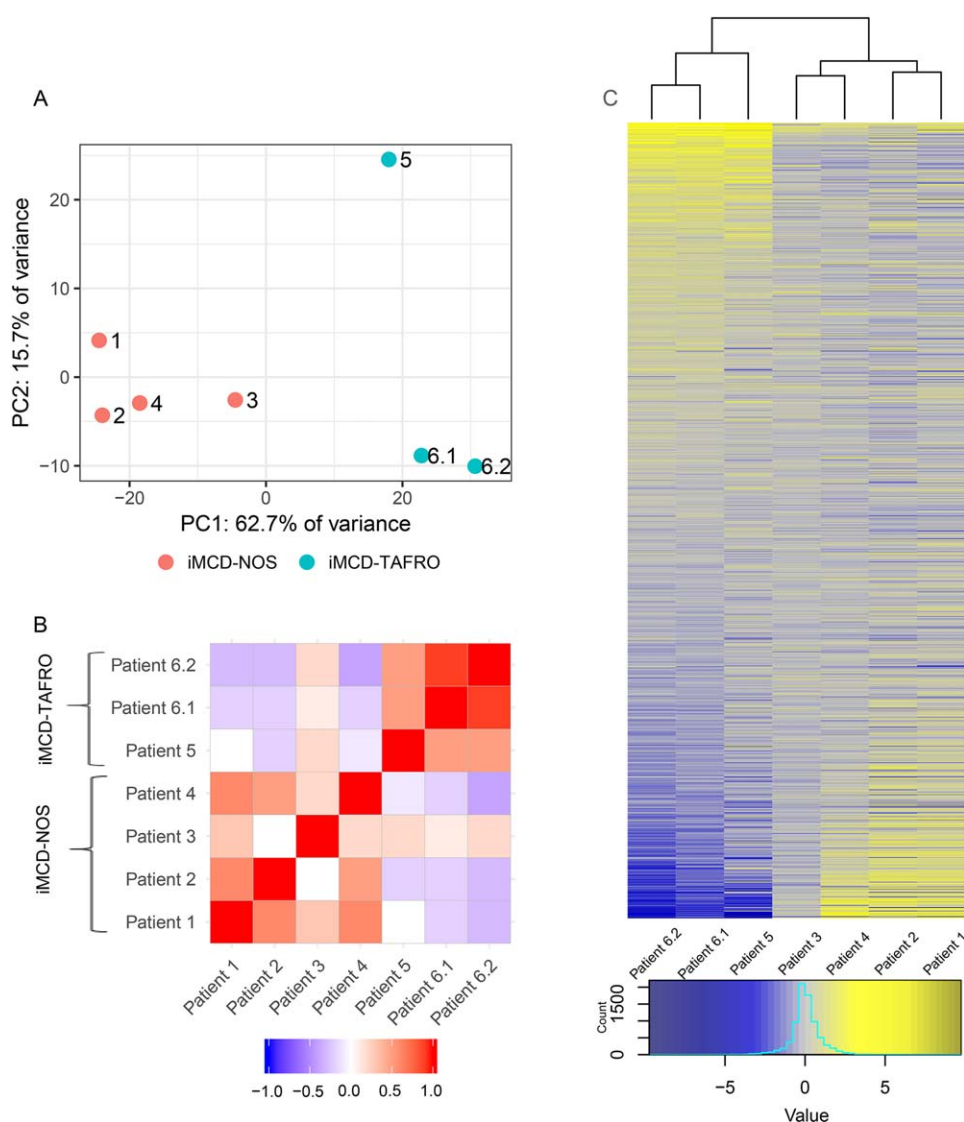
FIGURE 3 Two iMCD subgroups demonstrate unique proteomic profiles. (A) Principal component analysis of paired iMCD samples identifies two subgroups of patients by PC1 (62.7% of variance) that separate based on clinical subtype and response to anti-IL-6-therapy. (B) Pearson correlation plot shows positive correlation within the subgroups and negative correlation between the subgroups. (C). Heat map of all 1129 proteins demonstrates anti-correlation of many proteins; patients clustered together according to subgroup [Color figure can be viewed at wileyonlinelibrary.com]

correlated with the iMCD-NOS patients. We then visualized the relative values of all proteins in a heat map with unsupervised hierarchical clustering of paired samples (Figure 3C). iMCD-TAFRO and iMCD-NOS patients were separated on the first tier. Many of the most upregulated proteins in iMCD-TAFRO patients were downregulated in iMCD-NOS and vice versa (Supporting Information Table S7). Further, we performed a LIMMA modeling analysis on all proteins for iMCD-TAFRO and iMCD-NOS subgroups and plotted the results. Though no proteins reached statistical significance in the iMCD-NOS subgroup, 229 proteins were statistically significant after adjustment in the iMCD-TAFRO subgroup (Supporting Information Figure S1). These results demonstrate clear differences in proteomic profiles between groups of iMCD patients. However, it is unclear if this distinction is due to clinical subtypes and/or anti-IL-6 response.

3.6 | PI3K/Akt/mTOR identified as a potential targetable pathway in iMCD

To generate insights into potential signaling pathways, we performed gene-set and pathway analyses on the proteins with >2-fold-change separately for iMCD-TAFRO and iMCD-NOS groups (listing of proteins in Supporting Information Tables S8 and S9). To ensure that our results were not a product of enrichment among the 1129 analytes that were quantified, we compared results to the background of all SOMAscan® proteins. IPA ranked "Phosphoinositide 3-kinase (PI3K) signaling in B lymphocytes" in the top two canonical pathways for both clinical subgroups by P value. All of the top five ranked pathways for iMCD-TAFRO and iMCD-NOS were significant by $P < .001$ (Supporting Information Table S10). When KEGG gene-set analyses were performed on

TABLE 1 Top 20 nonduplicated compounds identified to downregulate proteins that are >2-fold upregulated during iMCD-TAFRO flare

Compound name	Class of drug	Combined score
GDC-0980	PI3K & mTOR inhibitor	47.5
GSK-1059615	PI3K & mTOR inhibitor	46.8
XMD-1150	Selective LRRK2 inhibitor	45.1
Neratinib	TKI (EGFR/HER2)	43.2
Nintedanib	TKI (VEGFR/PDGFR)	41.4
BIX-01294	Histone methyl transferase inhibitor	37.3
KIN001–244	PDK1 inhibitor	37.2
I-BET151	BET family inhibitor	37.0
Gefitinib	TKI (EGFR)	36.7
Trametinib	MEK inhibitor	36.0
XMD-892	BMK1/ERK5 inhibitor	35.3
AZD-6482	PI3K inhibitor	35.3
Geldanamycin	Benzoquinone Ansamycin Antibiotic	34.9
Celastrol	Triterpenoid antioxidant	34.7
Buparlisib	PI3K inhibitor	34.4
SAR-245408	PI3K inhibitor	34.1
GSK-1070916	Aurora B/C kinase inhibitor	33.2
Dasatinib	TKI (BCR/ABL and Src)	32.9
SB-239063	MAPK Inhibitor	32.8
NVP-BEZ235	PI3K & mTOR inhibitor	32.4

Proteins upregulated > 2-fold during iMCD-TAFRO flare were analyzed using the LINCS 1000 database. Six of the top 20 compounds identified to downregulate the upregulated proteins are of the PI3K & mTOR inhibitor class.

the iMCD-TAFRO cases, MAPK signaling and chemokine signaling were significantly enriched compared to background proteins ($P = .02$ and $P = .02$). PI3K-Akt was 1.22-fold enriched and had the third highest combined score, but did not meet significance when compared to background proteins ($P = .16$) (Supporting Information Table S11). For iMCD-NOS cases, KEGG gene-set analyses identified chemokine signaling and Vascular Endothelial Growth Factor (VEGF) signaling among the top five gene-sets, which were also significantly enriched over background (all $P < .01$) (Supporting Information Table S12). Lastly, we performed an enrichment analysis for compounds in the LINCS 1000 database that decrease gene expression of proteins with > 2-fold upregulation during flare among iMCD-TAFRO and iMCD-NOS cases. After multiple comparison adjustment, six of the 20 most significant compounds (highest combined score) identified to downregulate protein expression for iMCD-TAFRO patients were dual PI3K/mechanistic target of rapamycin (mTOR) inhibitors or PI3K inhibitors. The remaining 14 compounds each had different targets (Table 1). For iMCD-NOS patients, no compounds were identified below the false discovery rate to downregulate protein expression of the >2-fold upregulated

proteins. The identification of the PI3K/Akt/mTOR pathway across analyses performed on four separate gene-set databases suggest that it may be a novel therapeutic target for treating iMCD.

4 | DISCUSSION

Here, we have systematically characterized in a small patient cohort the breadth of soluble protein changes during iMCD flare in peripheral blood. Our results support the general model that iMCD flares involve a cytokine storm and acute inflammation. Acute phase reactants contributed strongly to the altered proteomic profile of patients in flare. NPS-PLA2, the only protein to meet statistical significance across all samples, has been found to be elevated in malignancies and inflammatory disorders and highly correlated with other inflammatory markers, including CRP and SAA.[25–28]

While iMCD has been described as an IL-6-driven lymphoproliferative disorder,[29] recent findings suggest that IL-6 is not the driving cytokine in all cases, and >50% of patients with iMCD do not respond to anti-IL6-therapy.[14] Our findings further indicate that iMCD pathogenesis is more complex than previously described. In our cohort, anti-IL-6-therapy induced a complete response in three of five patients in whom it was administered. However, the flare IL-6 levels were not highly upregulated compared to paired remission samples in these patients. When the anti-IL-6 treated samples were removed, we found that the degree of fold-change may have been underestimated. It is also possible that some patients may have dysregulation in IL-6 signaling such that small changes in IL-6 levels result in major downstream effects.[30] We previously found a significantly increased frequency of an IL-6 receptor polymorphism among iMCD patients (49%) compared to controls (33%). Individuals with this polymorphism expressed significantly higher levels of soluble IL-6 receptor, which we hypothesized could contribute to increased IL-6 activity through trans-signaling.[31]

A major finding in this study is that chemokines are significantly upregulated compared to interleukins and other cytokines during iMCD flare. These data suggest that the 'cytokine storm' described in iMCD would be more appropriately considered a 'chemokine storm.' The most upregulated circulating cytokine is the chemokine CXCL13, which is essential for lymph node development and B cell homing to germinal centers; upregulated levels of CXCL13 have been observed in disorders that overlap clinically and histopathologically with iMCD.[32–36] This finding is also notable given that two flare samples were collected from patients (patient 2 and 6, flare 1) while on rituximab, which has been shown to decrease serum CXCL13 levels and may have dampened CXCL13 fold-change between flare and remission.[37–39] CXCL13 levels were still more than 4-fold higher in flare compared to remission in those patients. Additionally, no patients received rituximab within 12 months of remission sample collection, so decreased remission sample CXCL13 is not expected. Thus, CXCL13 may have been further upregulated across patients if rituximab had not been administered during two patients' flare samples.

Consistent with proteomic data, we found increased germinal center CXCL13 staining in a diffuse, meshwork pattern in iMCD patients'

lymph node tissue compared with metastasis-free sentinel lymph nodes from breast cancer patients. Lymph node tissue from all six iMCD patients was collected at the time of diagnosis prior to any treatment administration, and therefore the observed CXCL13 is representative of the treatment-naive state of iMCD flare. CXCL13 is primarily secreted by FDCs and Tfh cells to home B cells into lymph node germinal centers (via CXCR5).[40] Diffuse, strong expression of CXCL13 on FDCs has been described in lymph node tissue from unicentric Castleman disease and HHV-8-positive MCD.[41] FDC prominence is frequently observed in iMCD,[5] and FDC dysplasia has been occasionally reported.[41–45] Similar to what is observed in iMCD, increased numbers of lymphoid follicles are seen in CXCL13 overexpressing mice.[32,46] However, the germinal centers in iMCD are typically small with few B cells and atrophic features, which is observed in CXCL13 knock-out mice. Overlap between the phenotype observed in these mice and the histopathological hallmarks of iMCD[47] suggest that there may be dysregulation of CXCL13 signaling in iMCD. Perhaps elevated CXCL13 secreted by FDCs could drive B cell maturation into plasma cells, which are increased in iMCD lymph nodes,[5] and could lead to auto-antibody producing plasma cells. Alternatively, the increased CXCL13 could represent increased, nonspecific germinal center activity,[40] which has been observed in related disorders,[32–36] or a normal response to the failure of B cells to populate the atrophic germinal centers.

CCL21 and CCL23 are also highly upregulated during iMCD flares and have functions directly relevant to lymphoid cell organization. Like CXCL13, CCL21 is a homeostatic chemokine produced by fibroblastic reticular cells, a type of lymph node stromal cell, that attracts dendritic cells and T cells to the T cell zone/interfollicular space and is essential for normal lymph node morphology, which is perturbed in iMCD. CCL23 attracts T cells and monocytes to sites of inflammation and promotes angiogenesis (via CCR1). Our results suggest that chemokine upregulation in lymph node stromal cells—and considering the meshwork staining pattern, FDC stromal cells, in particular—may contribute to iMCD pathogenesis and warrant further investigation.

Unexpectedly, we saw strong increases in the abundance of complement proteins during iMCD flares. Increases in complement factors have not been previously described in iMCD. C3b, the main effector molecule of the complement system, and its cleavage products C3a and C3a-des-arginine were among the most upregulated proteins in the iMCD-TAFRO cases. Auto-antibodies, which are present in approximately 30% of iMCD cases, can trigger complement activation when bound to self-antigen.[16] Future studies are required to determine complement's role in iMCD pathogenesis and will be an important area to explore given there is already a safe and effective anti-complement antibody in clinical use.[48]

Recently, Iwaki et al. quantified the levels of 18 serum cytokines from 11 iMCD-TAFRO patients in flare, 6 iMCD-NOS patients in flare, and 21 healthy controls.[15] Among the 18 cytokines measured by fluorescent bead immunoassay, there were 13 interleukins, 1 chemokine, and 4 other cytokines. All but one cytokine (IL-9) were among the 1129 analytes quantified in our study, and CXCL13 was not measured by Iwaki et al. They found significantly increased IL-10, IL-23, and VEGF-A in both iMCD-TAFRO and iMCD-NOS compared to healthy

controls. IL-10 and IL-23 were upregulated in iMCD-TAFRO in our study, but demonstrated minimal magnitude and inconsistent changes in iMCD-NOS. VEGF-A (VEGF-121) was greater than two-fold upregulated on average across all patients in our study. Elevated VEGF-A, which promotes cell survival, angiogenesis, and vascular permeability, has been previously described in iMCD,[16,49] and patients often demonstrate VEGF-related symptoms, such as highly vascularized lymph nodes, eruptive cherry hemangiomatosis,[50] and vascular leak syndrome.[5] Interestingly, IL-6 was not significantly increased in either the iMCD-TAFRO or iMCD-NOS groups compared to healthy controls in the Iwaki study.

The one chemokine measured by Iwaki et al, CXCL10 (or IFN-γ-Inducible Protein 10 (IP-10), was the only cytokine significantly higher in iMCD-TAFRO flare compared with both iMCD-NOS flare and healthy controls. Though CXCL10 was only the 18th most-upregulated cytokine on average across patients in our study, iMCD-TAFRO patients demonstrated >50% upregulation of CXCL10. Like CCL23, which was highly upregulated in our study, CXCL10 plays an important role in the recruitment of T cells to sites of inflammation.

Iwaki et al. also found that platelet-derived growth factor subunit A (PDGF-AA), which is released upon platelet activation,[15,51] was the only cytokine significantly lower in iMCD-TAFRO compared with controls. There was also a trend toward decreased PDGF-AA in iMCD-TAFRO compared to iMCD-NOS $(P = .09)$.[15] PDGF-AA was likewise > 2-fold downregulated in iMCD-TAFRO and >2-fold upregulated in iMCD-NOS in our study. PDGF-AA has been found to be elevated in immune/idiopathic thrombocytopenic purpura (ITP), in whom the thrombocytopenia is caused by peripheral thrombocyte consumption.[52] The etiology of the thrombocytopenia in iMCD-TAFRO is not known. Though iMCD-TAFRO and ITP share similar clinical features, including thrombocytopenia and megakaryocyte hyperplasia, the divergent PDGF-AA levels suggest that there may be different mechanisms involved in the thrombocytopenia in these disorders.[15] Despite differences in assays, sample types, and comparison groups, there were several consistent findings between these studies, such as significant differences between iMCD-TAFRO and iMCD-NOS.

We observed striking differences between patient proteomes from the two groups that associated with iMCD-TAFRO and iMCD-NOS. In our study, these groups also associated with response to anti-IL6-therapy. Notably, over 200 proteins were significantly upregulated or downregulated after adjustment in the iMCD-TAFRO group, which would be expected considering the high correlation between patients, while no proteins in the iMCD-NOS group met significance. Both iMCD-TAFRO patients were anti-IL-6 nonresponders and all three iMCD-NOS patients treated with anti-IL-6-therapy responded. Importantly, there have been reports of iMCD-TAFRO cases that have responded to anti-IL-6-therapy[53–59] and others that have not.[50,60–66] The proteomic differences between the two groups may represent differences between clinical subtypes or be a signature of anti-IL-6 response. In either case, the most upregulated proteins and enriched signaling pathways may constitute therapeutic targets.

PI3K, a key member of the PI3K/Akt/mTOR signaling pathway, was identified as a top canonical pathway in both subgroups, and six

inhibitors of PI3K/Akt/mTOR signaling were identified in the top twenty compounds predicted to downregulate expression of upregulated proteins in iMCD-TAFRO patients. PI3K/Akt/mTOR is a key regulator of angiogenesis, lymphoproliferation, and inflammation that is therapeutically targetable. Results suggesting involvement of the PI3K/Akt/mTOR pathway were consistently significant across the different pathway and gene-set databases, strengthening our finding that the PI3K/Akt/mTOR signaling pathway may be a rational treatment target for anti-IL-6 nonresponders.

A major limitation of this study is the small number of patient samples analyzed. Though our decision to include only iMCD patients with matched flare and remission samples limited the number of eligible patients with this rare disease, we wanted to identify proteomic changes that can be attributed to disease state and therapies. We expect that the continued growth of the international, multi-center Castleman Disease Collaborative Network,[67] which was started in 2012, will be instrumental in recruitment of larger numbers of patients with this rare disease for future translational studies. Furthermore, while large-scale plasma protein profiling gives a systematic view of protein changes, this approach may overlook highly potent proteins where small changes in concentration result in major biological effects as well as nonsecreted factors, which were not assayed. Given the exploratory nature of the analysis, there is also the potential for false discovery. Therefore, we employed a false discovery rate and performed gene-set enrichment analyses to improve our power for identifying significantly enriched or depleted groups of genes. Another limitation of this study is that renal dysfunction affects excretion of circulating proteins, particularly small (<25 kDa) proteins,[68] and three patients (2, 5, 6) experienced borderline or elevated creatinine suggestive of renal dysfunction during flare. Decreased excretion may therefore have contributed to increased concentration of some proteins, though these increased proteins may also contribute to iMCD pathophysiology. Further, treatments, such as anti-IL-6 therapies (siltuximab and tocilizumab), rituximab, corticosteroids, and chemotherapies may affect the plasma proteome. We addressed the potential effects of anti-IL-6 therapy and rituximab and provided each of the treatments administered to these patients. None of the major observations in this study segregated to only patients on rituximab, corticosteroids, or chemotherapies, and other than those discussed, we are not aware of any specific effects of these agents on the noted proteins. Lastly, the lack of samples from a healthy control population prevent comparison of disease state from both flare and remission with otherwise healthy controls. However, we sought to identify proteomic changes occurring within individuals between flare and remission. Comparisons between iMCD flare samples and healthy controls can introduce inter-individual differences in plasma proteomes that can make changes difficult to interpret.

Despite these limitations our study provides insights into the pathogenesis of iMCD, including identification of a 'chemokine storm' associated with iMCD flares and potential involvement of lymph node stromal cells. Additionally, our studies reveal the proteomic differences between flare and remission and the potential to molecularly define iMCD subgroups. Future studies testing the contribution of individual disease mediators will be critical to building a better understanding of iMCD and leading the field to better treatments.

ORCID

David C. Fajgenbaum http://orcid.org/0000-0002-7367-8184

REFERENCES

[1] Munshi N, Mehra M, van de Velde H, et al. Use of a claims database to characterize and estimate the incidence rate for Castleman disease. *Leuk Lymphoma.* 2015;56(5):1252–1260.

[2] Dispenzieri A, Armitage JO, Loe MJ, et al. The clinical spectrum of Castleman's disease. *Am J Hematol.* 2012;87(11):997–1002.

[3] Shin D-Y, Jeon YK, Hong Y-S, et al. Clinical dissection of multicentric Castleman disease. *Leuk Lymphoma.* 2011;52(8):1517–1522.

[4] Melikyan AL, Egorova EK, Kovrigina AM, et al. Clinical and morphological features of different types of Castleman's disease]. *Ter Arkh.* 2015;87(7):64–71. [

[5] Fajgenbaum DC, Uldrick TS, Bagg A, et al. International, evidence-based consensus diagnostic criteria for HHV-8-negative/idiopathic multicentric Castleman disease. *Blood.* 2017;129(12):1646–1657.

[6] Iwaki N, Fajgenbaum DC, Nabel CS, et al. Clinicopathologic analysis of TAFRO syndrome demonstrates a distinct subtype of HHV-8-negative multicentric Castleman disease. *Am J Hematol.* 2016;91(2): 220–226.

[7] Masaki Y, Kawabata H, Takai K, et al. Proposed diagnostic criteria, disease severity classification and treatment strategy for TAFRO syndrome, 2015 version. *Int J Hematol.* 2016;103(6):686–692.

[8] Srkalovic G, Marijanovic I, Srkalovic MB, Fajgenbaum DC. TAFRO syndrome: new subtype of idiopathic multicentric castleman disease. *Bosn J Basic Med Sci.* 2017;17(2):81–84.

[9] Uldrick TS, Polizzotto MN, Yarchoan R. Recent advances in Kaposi sarcoma herpesvirus-associated multicentric Castleman disease. *Curr Opin Oncol.* 2012;24(5):495–505.

[10] Tisoncik JR, Korth MJ, Simmons CP, et al. Into the eye of the cytokine storm. *Microbiol Mol Biol Rev.* 2012;76(1):16–32.

[11] Yoshizaki K, Matsuda T, Nishimoto N, et al. Pathogenic significance of interleukin-6 (IL-6/BSF-2) in Castleman's disease. *Blood.* 1988;10 (4):13–17.

[12] Casper C, Chaturvedi S, Munshi N, et al. Analysis of inflammatory and anemia-related biomarkers in a randomized, double-blind, placebo-controlled study of siltuximab (anti-IL6 monoclonal antibody) in patients with multicentric castleman disease. *Clin Cancer Res.* 2015;21(19):4294–42304.

[13] Nishimoto N, Kanakura Y, Aozasa K, et al. Humanized anti-interleukin-6 receptor antibody treatment of multicentric Castleman disease. *Blood.* 2005;106(8):2627–2632.

[14] van Rhee F, Wong RS, Munshi N, et al. Siltuximab for multicentric Castleman's disease: a randomised, double-blind, placebo-controlled trial. *Lancet Oncol.* 2014;15(9):966–974.

[15] Iwaki N, Gion Y, Kondo E, et al. Elevated serum interferon γ-induced protein 10 kDa is associated with TAFRO syndrome. *Sci Rep.* 2017;7:42316. (January):

[16] Liu AY, Nabel CS, Finkelman BS, et al. Idiopathic multicentric Castleman's disease: a systematic literature review. *Lancet Haematol.* 2016;3(4):e163–e175.

[17] Gold L, Ayers D, Bertino J, et al. Aptamer-based multiplexed proteomic technology for biomarker discovery. *PLoS One.* 2010;5(12): e15004.

[18] R Core Team. R: a Language and Environment for Statistical Computing. Vienna, Austria: R Foundation for Statistical Computing; 2017.

[19] Smyth GK, Michaud J, Scott HS. Use of within-array replicate spots for assessing differential expression in microarray experiments. *Bioinformatics.* 2005;21(9):2067–2075.

[20] Benjamini Y, Hochberg Y. Controlling the false discovery rate: a practical and powerful approach to multiple testing. *J R Stat Soc B.* 1995;57(1):289–300.

[21] Chen EY, Tan CM, Kou Y, et al. Enrichr: interactive and collaborative HTML5 gene list enrichment analysis tool. *BMC Bioinformatics.* 2013;14:128.

[22] Kuleshov MV, Jones MR, Rouillard AD, et al. Enrichr: a comprehensive gene set enrichment analysis web server 2016 update. *Nucleic Acids Res.* 2016;44(W1):W90–W97.

[23] Fajgenbaum DC, Van Rhee F, Nabel CS. HHV-8-negative, idiopathic multicentric Castleman disease: novel insights into biology, pathogenesis, and therapy. *Blood.* 2014;123(19):2924–2933.

[24] Nishimoto N, Terao K, Mima T, et al. Mechanisms and pathologic significances in increase in serum interleukin-6 (IL-6) and soluble IL-6 receptor after administration of an anti-IL-6 receptor antibody, tocilizumab, in patients with rheumatoid arthritis and Castleman disease. *Blood.* 2008;112(10):3959–3964.

[25] Menschikowski M, Hagelgans A, Schuler U, et al. Plasma levels of phospholipase A2-IIA in patients with different types of malignancies: prognosis and association with inflammatory and coagulation biomarkers. *Pathol Oncol Res.* 2013;19(4):839–846.

[26] Menschikowski M, Hagelgans A, Fuessel S, et al. Serum amyloid A, phospholipase A2-IIA and C-reactive protein as inflammatory biomarkers for prostate diseases. *Inflamm Res.* 2013;62(12):1063–1072.

[27] Sullivan CP, Seidl SE, Rich CB, Raymondjean M, Schreiber BM. Secretory phospholipase A$_2$, Group IIA is a novel serum amyloid a target gene. *J Biol Chem.* 2010;285(1):565–575.

[28] Uusitalo-Seppälä R, Peuravuori H, Koskinen P, Vahlberg T, Rintala EM. Role of plasma bactericidal/permeability-increasing protein, group IIA phospholipase A$_2$, C-reactive protein, and white blood cell count in the early detection of severe sepsis in the emergency department. *Scand J Infect Dis.* 2012;44(9):697–704.

[29] El-Osta HE, Kurzrock R. Castleman's disease: from basic mechanisms to molecular therapeutics. *Oncologist.* 2011;16(4):497–511.

[30] Patel M, Ikeda S, Pilat SR, Kurzrock R. JAK1 genomic alteration associated with exceptional response to siltuximab in cutaneous castleman disease. *JAMA Dermatol.* 2017;153(5):449–452.

[31] Stone K, Woods E, Szmania SM, et al. Interleukin-6 receptor polymorphism is prevalent in HIV-negative Castleman disease and is associated with increased soluble interleukin-6 receptor levels. *PLoS One.* 2013;8(1):e54610.

[32] Klimatcheva E, Pandina T, Reilly C, et al. CXCL13 antibody for the treatment of autoimmune disorders. *BMC Immunol.* 2015;16(1):6–6.

[33] Kramer JM, Klimatcheva E, Rothstein TL. CXCL13 is elevated in Sjögren's syndrome in mice and humans and is implicated in disease pathogenesis. *J Leukoc Biol.* 2013;94(5):1079–1089.

[34] Barone F, Bombardieri M, Manzo A, et al. Association of CXCL13 and CCL21 expression with the progressive organization of lymphoid-like structures in Sjögren's syndrome. *Arthritis Rheum.* 2005;52(6):1773–1784.

[35] Dunleavy K, Wilson WH, Jaffe ES. Angioimmunoblastic T cell lymphoma: pathobiological insights and clinical implications. *Curr Opin Hematol.* 2007;14(4):348–353.

[36] Dupuis J, Boye K, Martin N, et al. Expression of CXCL13 by neoplastic cells in angioimmunoblastic T-cell lymphoma (AITL): a new diagnostic marker providing evidence that AITL derives from follicular helper T cells. *Am J Surg Pathol.* 2006;30(4):490–494.

[37] Pranzatelli MR, Tate ED, Travelstead AL, Verhulst SJ. Chemokine/cytokine profiling after rituximab: reciprocal expression of BCA-1/CXCL13 and BAFF in childhood OMS. *Cytokine.* 2011;53(3):384–389.

[38] Rosengren S, Wei N, Kalunian KC, Kavanaugh A, Boyle DL. CXCL13: a novel biomarker of B-cell return following rituximab treatment and synovitis in patients with rheumatoid arthritis. *Rheumatology.* 2011;50(3):603–610.

[39] Alvarez E, Piccio L, Mikesell RJ, et al. Predicting optimal response to B-cell depletion with rituximab in multiple sclerosis using CXCL13 index, magnetic resonance imaging and clinical measures.

[40] Havenar-Daughton C, Lindqvist M, Heit A, et al. CXCL13 is a plasma biomarker of germinal center activity. *Proc Natl Acad Sci USA.* 2016;113(10):2702–2707.

[41] Vermi W, Lonardi S, Bosisio D, et al. Identification of CXCL13 as a new marker for follicular dendritic cell sarcoma. *J Pathol.* 2008;216 (3):356–364.

[42] Chang K-C, Wang Y-C, Hung L-Y, et al. Monoclonality and cytogenetic abnormalities in hyaline vascular Castleman disease. *Mod Pathol.* 2014;27(6):823–831.

[43] Yasuda S, Tanaka K, Ichikawa A, et al. Aggressive TAFRO syndrome with reversible cardiomyopathy successfully treated with combination chemotherapy. *Int J Hematol.* 2016;104(4):512–518.

[44] Inoue M, Ankou M, Hua J, et al. Complete resolution of TAFRO syndrome (thrombocytopenia, anasarca, fever, reticulin fibrosis and organomegaly) after immunosuppressive therapies using corticosteroids and cyclosporin A : a case report. *J Clin Exp Hematop.* 2013;53 (1):95–99.

[45] Sun X, Chang K-C, Abruzzo LV, et al. Epidermal growth factor receptor expression in follicular dendritic cells: a shared feature of follicular dendritic cell sarcoma and Castleman's disease. *Hum Pathol.* 2003;34(9):835–840.

[46] Ansel KM, Ngo VN, Hyman PL, et al. A chemokine-driven positive feedback loop organizes lymphoid follicles. *Nature.* 2000;406(6793): 309–314.

[47] Cronin DMP, Warnke RA. Castleman disease - An update on classification and the spectrum of associated lesions. *Adv Anat Pathol.* 2009;16(4):236–246.

[48] Hillmen P, Young NS, Schubert J, et al. The complement inhibitor eculizumab in paroxysmal nocturnal hemoglobinuria. *N Engl J Med.* 2006;355(12):1233–1243.

[49] Nishi J, Arimura K, Utsunomiya A, et al. Expression of vascular endothelial growth factor in sera and lymph nodes of the plasma cell type of Castleman's disease. *Br J Haematol.* 1999;104(3):482–485.

[50] Fajgenbaum DC, Fajgenbaum D, Rosenbach M, et al. Eruptive cherry hemangiomatosis associated with multicentric Castleman disease: a case report and diagnostic clue. *JAMA Dermatol.* 2013;149(2):204–208.

[51] Kaplan DR, Chao FC, Stiles CD, Antoniades HN, Scher CD. Platelet alpha granules contain a growth factor for fibroblasts. *Blood.* 1979;53(6):1043–1052.

[52] Katoh O, Kimura A, Fujimura K, Kuramoto A. Progression activity for platelet-derived growth factor in plasma of patients with idiopathic thrombocytopenic purpura and aplastic anemia. *Nippon Ketsueki Gakkai Zasshi.* 1989;52(1):113–117.

[53] Sakai K, Maeda T, Kuriyama A, et al. TAFRO syndrome successfully treated with tocilizumab: a case report and systematic review. *Mod Rheumatol.* 2016;1–6.

[54] Fujiwara S, Mochinaga H, Nakata H, et al. Successful treatment of TAFRO syndrome, a variant type of multicentric Castleman disease with thrombotic microangiopathy, with anti-IL-6 receptor antibody and steroids. *Int J Hematol.* 2016;103(6):718–723.

[55] Sakashita K, Murata K, Inagaki Y, Oota S, Takamori M. An anterior mediastinal lesion in TAFRO syndrome showing complete remission after glucocorticoid and tocilizumab therapy. *Respirol Case Rep.* 2016;4(5):e00173.

[56] Kubokawa I, Yachie A, Hayakawa A, et al. The first report of adolescent TAFRO syndrome, a unique clinicopathologic variant of multicentric Castleman's disease. *BMC Pediatr.* 2014;14(1):139.

[57] Kawabata H, Kotani S, Matsumura Y, et al. Successful treatment of a patient with multicentric Castleman's disease who presented with thrombocytopenia, ascites, renal failure and myelofibrosis using tocilizumab, an anti-interleukin-6 receptor antibody. *Intern Med.* 2013;52(13):1503–1507.

[58] Coutier F, Meaux Ruault N, Crepin T, et al. A comparison of TAFRO syndrome between Japanese and non-Japanese cases: a case report and literature review. *Ann. Hematol.* 2018;97:401–407.

[59] Fujiki T, Hirasawa S, Watanabe S, Iwamoto S, Ando R. Successful treatment by tocilizumab without steroid in a very severe case of TAFRO syndrome. *CEN Case Rep.* 2017;6(1):105–110. 0

[60] Konishi Y, Takahashi S, Nishi K, et al. Successful treatment of TAFRO syndrome, a Variant of Multicentric Castleman's disease, with cyclosporine a: possible pathogenetic contribution of Interleukin-2. *Tohoku J Exp Med.* 2015;236(4):289–295.

[61] Tadokoro A, Kanaji N, Hara T, et al. An Uncharted Constellation: TAFRO Syndrome. *Am J Med.* 2016;129(9):938–941.

[62] Tatekawa S, Umemura K, Fukuyama R, et al. Thalidomide for tocilizumab-resistant ascites with TAFRO syndrome. *Clin Case Rep.* 2015;3(6):472–478.

[63] Simons M, Apor E, Butera JN, Treaba DO. TAFRO syndrome associated with EBV and successful triple therapy treatment: case report and review of the literature. *Case Rep Hematol.* 2016;2016:1.

[64] Tedesco S, Postacchini L, Manfredi L, et al. Successful treatment of a Caucasian case of multifocal Castleman's disease with TAFRO syndrome with a pathophysiology targeted therapy - a case report. *Exp Hematol Oncol.* 2015;4(1):3.

[65] Hiramatsu S, Ohmura K, Tsuji H, et al. Successful treatment by rituximab in a patient with TAFRO syndrome with cardiomyopathy. *Jpn J Clin Immun.* 2016;39(1):64–71.

[66] Tanaka H, Bujo S, Itobayashi E, et al. TAFRO syndrome with a rapid fatal course despite corticosteroid and tocilizumab therapy. *J Hematopathol.* 2016;9(4):167–171.

[67] Fajgenbaum D, Ruth J, Kelleher D, Rubenstein A. The collaborative network approach: a new framework to accelerate Castleman's disease and other rare disease research. *Lancet Haematol.* 2016;3(4):e150–e175.

[68] Mehan MR, Ostroff R, Wilcox SK, et al. Highly multplexed proteomic platform for biomarker discovery, diagnostics, and therapeutics. *Complement Ther.* 2013;283–300.

SUPPORTING INFORMATION

Additional Supporting Information may be found online in the supporting information tab for this article.